Speed Interference Suppression for PD Radar Based on Adaptive Dictionary

Zhe Du[1], Lexin Yu[2], Jin Zhang[1], Mingjuan Cai[3], and Tao Jiang[2]

[1]Shanghai Electro-Mechanical Engineering Institute
Shanghai 201109, China
dudo1987@163.com, zoey0041@163.com

[2]College of Information & Communication Engineering
Harbin Engineering University, Harbin 150001, China
yulexing@hrbeu.edu.cn, jiangtao@hrbeu.edu.cn

[3]Naval Research Academy
Shanghai 200235, China
dudo1987@163.com

Abstract – Random pulse initial phase (RPIP) signal is a kind of agility waveform which is commonly used in pulse Doppler (PD) radar. Although RPIP has the merit of restraining velocity deception jamming effectively, its efficiency is restricted under the condition of strong interference. To make the RPIP signal fully play the anti-jamming performance, this paper proposed a speed interference suppression method based on adaptive dictionar that separates the target echo from the strong jamming signal with good sparsity. First, the prior knowledge of strong interference signal is obtained by the technique of peak detection which is combined with the dual channel processing. Second, the quasi-Karhunen-Loeve transform (Q-KLT) basis of interference signal is constructed based on the prior knowledge, and the approximate Q-KLT basis of target signal is constructed by the way of dictionary learning, and those signals can be obtained from the adaptive dictionary by the algorithm of base tracking (BP). Finally, the effectiveness of the proposed method is verified by numerical simulation, which proves that the method can ensure a lower Doppler sidelobe in the strong interference scene, which confirmed that it has a good anti-velocity deception performance.

Index Terms – speed deception jamming, anti-jamming, sparse decomposition, dictionary learning, KLT basis

I. INTRODUCTION

Pulse Doppler (PD) radar is one kind of radar system that adopted moving target detection (MTD) technology to detect targets in noise, clutter, and interference. It plays an important role in air reconnaissance, ground moving target recognition, and air traffic control [1, 2]. In the electronic countermeasures (ECM) scenario, PD radar often suffers from the serious threat of radar active jamming [3]. Especially, with the development of digital radio frequency memory (DRFM), active deception jamming with diversity and strong antagonism seriously reduced the performance of PD radar detection [4–6].

In recent years, to protect PD radar from the velocity deception jamming, sparse decomposition and compressed sensing have been applied to the field of radar anti-jamming. They can separate the signals of target and jamming from the echo and realize the suppression of active deception jamming. Literature [7] constructed an over-complete dictionary to match the signal and used the sparse decomposition to suppress the smeared spectrum (SMSP) jamming. For the detection and recognition of velocity false target interference, literature [8] established a combination dictionary of true targets and false targets, and then used compressed sensing to realize the recognition of target and interference. On the basis of [8], literature [9] constructed a composite dictionary and a short-time sparse recovery method to suppress translational velocity interference and micro-motion velocity jamming. It is worth noting that the method of dictionary design is adopted in literature [8, 9] to construct a dictionary. Because the dictionary constructed by this method is independent of the input signal and has no adaptability, the sparsity of the signal under this fixed dictionary is weak; so they only can recognize and suppress jamming under the weak interference intensity. In this paper, an adaptive dictionary is proposed to suppress strong speed interference.

Before constructing the adaptive dictionary of jamming signal, it is necessary to obtain the Doppler information of jamming as the prior knowledge of the

Submitted On: January 16, 2021
Accepted On: December 4, 2021

https://doi.org/10.13052/2022.ACES.J.370313

sparse domain. It can be seen from [10] and [11] that multi-channel processing technology can obtain Doppler information, but there are some problems in it, such as complex device design and low device utilization. Based on the improvement of this technology, the peak detection method proposed can estimate the pulse repetition interval (PRI) number i of jamming signal lagging radar. Then dual channels are enough to achieve the acquisition of Doppler information and it is the reason why this method is named as dual channel processing technology.

On completing the mission of obtaining the Doppler information of jamming, the method of constructing adaptive dictionary is analyzed. The basic idea is that to construct the quasi-Karhunen-Loeve transform (Q-KLT) basis of the jamming based on the prior knowledge, which enables the strong jamming signal to have good sparsity under its adaptive dictionary. Aiming at the establishment of adaptive dictionary of target signal, the approximate Q-KLT basis is constructed by the method of dictionary learning. Dictionary learning is another effective method to construct a dictionary to find the optimal set of atoms of a certain kind of signal by iteration. Here, these atoms can well reflect the characteristics of such signals and they can describe those signals most sparsely. In this paper, the orthogonal matching pursuit (OMP) algorithm is adopted to find the best sparsity atom in the pre-construction dictionary of the target signal, and the corresponding matching coefficient is calculated. Then the extracted atoms are combined into a template, and the matching coefficient is used to construct the approximate Q-KLT basis of the target signal. Finally, base tracking (BP) algorithm is used to separate the target and jamming, which can suppress the velocity deception jamming.

The main contents of the rest of this paper are as follows. In the second section, the dual channel processing is described to obtain prior knowledge which is based on the peak detection. In the third section, the adaptive Q-KLT basis is constructed to separate the target and jamming. In the fourth section, simulation result is given.

II. ACQUISITION OF PRIOR KNOWLEDGE

In our previous work, "Dictionary Learning and Waveform Design for Dense False Target Jamming Suppression" (DOI: 10.47037/2021.ACES.J.360908), the peak detection method is proposed to estimate the phase difference of adjacent pulse compression (PC) signals and realizes the detection of radar active deception jamming, which is based on wavelet transform algorithm. In this paper, the peak detection is used to estimate the PRI number i of jamming signal lagging radar signal, and the prior knowledge is obtained by combining the dual channel processing. The output results of matched filtering in the coherent processing interval (CPI) are rewritten into PC signals in the slow time domain. The signal expression is

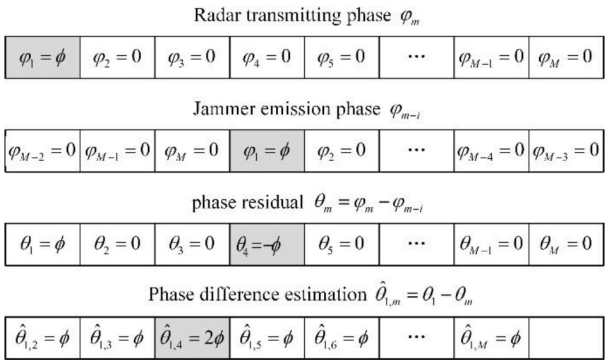

Fig. 1. Schematic diagram of estimated jamming delay i.

$$y(m)=\sum_{p=1}^{P}\tilde{\sigma}_T^p e^{j2\pi f_T^p mT_r}+e^{j\theta(m)}\cdot\sum_{q=1}^{Q}\tilde{\sigma}_J^q e^{j2\pi f_J^q mT_r}+V(m) \tag{1}$$

where T_r is the pulse repetition period, and P and Q are the number of target and interference, respectively. σ_T^p and f_T^p are the amplitude and Doppler frequency of the pth (p = 1, 2,…,P) target, respectively. σ_J^p and f_J^p are the amplitude and Doppler frequency of the qth (q = 1, 2,…,Q) target, respectively. $\theta(m)$ is the phase residual of the signal and $V(m)$ is the Gaussian white noise.

The estimation of jamming delay i based on peak detection is explained in Figure 1. The radar transmits a set of initial phase waveform of quasi-random pulse in CPI. The initial phase of the first pulse in the waveform aggregate is set to $\varphi_1=\phi$, while the initial phase of other pulse is $\varphi_m=0(m=2,\ldots,M)$. Assuming that i is 3 which is the number of PRI of the jamming, the initial phase of the fourth pulse in the random pulse initial phase (RPIP) waveform set sent by the jammer is $\varphi_4=\phi$. Then the phase residuals of the first pulse and the fourth pulse are $\theta_1=\phi$ and $\theta_4=-\phi$, respectively. Finally, the peak detection is used to estimate the phase difference between the first PC peak and the following $M-1$ PC peak. The phase difference estimated in the third detection is $\hat{\theta}_{1,3}=2\phi$, while the other phase difference is estimated to be $\hat{\theta}_{1,m}=\varphi(m\neq 3)$. Then, the number of PRI of the jamming signal sent by the jammer is determined to be 3. Based on the several kinds of quasi-random initial phase pulse set and the peak detection, the jamming delay i value can be determined, which improves the complexity of device design in multi-channel processing.

As an alternative, the Doppler information of target and jamming can be obtained by two channels, which

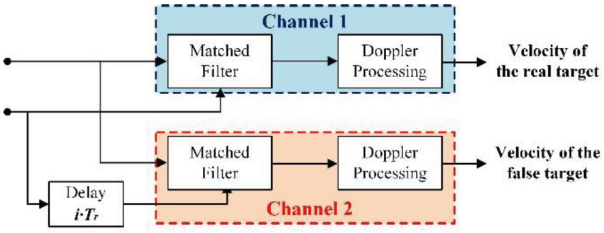

Fig. 2. Technical diagram of dual channel processing.

is called dual channel processing technology. Figure 2 shows the schematic diagram of dual channel processing technology. In channel one, the mth radar echo has the matching coefficient of $p_m^*(-t)$. The output of matched filter is described by eqn. (1), which is $y^{\text{channel 1}}(m) = y(m)$. The mth radar echo in channel two passes through the matched filter with the matching coefficient of $p_{m-i}^*(-t)$. And the output is

$$y^{\text{channel2}}(m) = e^{j\theta(m)} \sum_{p=1}^{P} \tilde{\sigma}_T^p e^{j2\pi f_T^p m T_r} + \sum_{q=1}^{Q} \tilde{\sigma}_J^q e^{j2\pi f_J^q m T_r} + V(m). \quad (2)$$

From eqn. (2), we can get that due to the influence of phase residual θ_m, and the energy of target diffuses to the whole Doppler spectrum. However, the phase cancelation of the jamming forms a peak on the Doppler spectrum; so the Doppler frequency of the peak can be obtained on channel two.

III. ADAPTIVE DICTIONARY AGAINST SPEED JAMMING

The main idea of single channel separation algorithm is to separate the mixed signals in sparse domain first and then recover the separated signals in time domain. The selection and construction of the dictionary (basis function) determines the sparsity of the signal, which is the most important step for the separation of the target and the jamming. In this section, we will introduce the method of building adaptive dictionary and the detail process.

A. Pre-construction of target signal dictionary

Usually, the target velocity is not fuzzy in the traditional sense and it can be divided into $N(N \geq M)$ parts to get the velocity resolution unit $\Delta v = \lambda / (2NT)$, where λ is the wavelength.

If the velocity of the target detected by the radar can be expressed as $v_n = (n-1)\Delta v$, $n = 1,2,\ldots,N$, then the Doppler frequency can be expressed as

$$f_n = \frac{2v_n}{\lambda} = \frac{n-1}{NT_r}. \quad (3)$$

If $v'(n) = (n-1)/N$, the target pre-constructed in the slow time domain can be expressed as

$$y_T(n,m) = \exp\left(j2\pi m v'(n)\right). \quad (4)$$

In order to simplify the expression, eqn. (4) is written as a vector $\boldsymbol{y}_{T,n}$, where $\boldsymbol{y}_{T,n}$ is a column vector of $M \times 1$.

The Doppler spectrum $\boldsymbol{y}_{T,n}$ of the target is obtained by discrete Fourier transform (DFT) of $\boldsymbol{Y}_{T,n}$ which is used as the atom $\boldsymbol{a}_{Y_T}^n = \boldsymbol{Y}_{T,n} = \text{FFT}\left[\boldsymbol{y}_{T,n}\right]$ in the pre-constructed target dictionary.

Atom $\boldsymbol{a}_{Y_T}^n$ is defined as the element of dictionary $\boldsymbol{A}_{Y_T} = \left[\boldsymbol{a}_{Y_T}^1, \boldsymbol{a}_{Y_T}^2, \ldots, \boldsymbol{a}_{Y_T}^N\right]$, and atom $\boldsymbol{g}_{Y_T}^n$ is defined as the diagonal vector of auto-correlation matrix of atom $\boldsymbol{a}_{Y_T}^n$, which has the expression as follows:

$$\boldsymbol{g}_{Y_T}^n = \text{diag}\left(\boldsymbol{a}_{Y_T}^n \left(\boldsymbol{a}_{Y_T}^n\right)^T\right), \quad n = 1,2,\ldots,N. \quad (5)$$

Atom $\boldsymbol{g}_{Y_T}^n$ is normalized to $\bar{\boldsymbol{g}}_{Y_T}^n$, and atom $\bar{\boldsymbol{g}}_{Y_T}^n$ is defined as the element of the normalized dictionary $\boldsymbol{G}_{Y_T} = \left[\bar{\boldsymbol{g}}_{Y_T}^1, \bar{\boldsymbol{g}}_{Y_T}^2, \ldots, \bar{\boldsymbol{g}}_{Y_T}^N\right]$.

B. Construction of adaptive Q-KLT basis

(a) Q-KLT basis of jamming signal

According to the prior knowledge obtained in the previous section, the jamming $y_J(m)$ in the slow time domain can be constructed, and its expression is defined as follows:

$$y_J(m) = \sum_{q=1}^{Q} \exp\left(j2\pi f_J^q m T_r + j\theta(m)\right). \quad (6)$$

In order to simplify the jamming expression, eqn. (6) is written in vector form $\boldsymbol{y}_J$, which is a column vector of $M \times 1$. Then $\boldsymbol{Y}_J$ can be gotten from $\boldsymbol{y}_J$ by DFT, and the auto-correlation $\boldsymbol{R}_{Y_J} = \text{E}\left\{\boldsymbol{Y}_J \boldsymbol{Y}_J^H\right\}$ of jamming signal in Doppler spectrum cabe calculated. Because $\boldsymbol{R}_{Y_J}$ is Hermitian matrix and a positive definite matrix, there must exist an orthogonal matrix $\boldsymbol{U}_{Y_J}$, which satisfied $\boldsymbol{U}_{Y_J} \boldsymbol{R}_{Y_J} \boldsymbol{U}_{Y_J}^H = \Lambda_{Y_J}$, where Λ_{Y_J} is a diagonal matrix with m eigenvalues of $\boldsymbol{R}_{Y_J}$.

(b) Approximation of Q-KLT basis for target signal

In the presence of velocity false target jamming, the mixed signal received can be regarded as the linear combination of target and jamming, and then the mixed Doppler spectrum signal $\tilde{\boldsymbol{Y}}$ can be obtained through the coherent processing. Suppose that $\boldsymbol{d}_{R_{\tilde{Y}}}$ is the diagonal vector of auto-correlation matrix of mixed signal $\tilde{\boldsymbol{Y}}$, which is the diagonal vector of $\boldsymbol{R}_{\tilde{Y}}$:

$$\boldsymbol{d}_{R_{\tilde{Y}}} = \text{diag}\left(\boldsymbol{R}_{\tilde{Y}}\right) = \text{diag}\left(\tilde{\boldsymbol{Y}} \tilde{\boldsymbol{Y}}^H\right). \quad (7)$$

Then, the optimal atom of the target is extracted by the OMP iterative algorithm. Among them, the OMP algorithm was originally proposed by Pati [12], which is used to calculate the sparse coefficient of signal under a certain transformation basis or an over-complete dictionary, so as to express the signal with as few atoms as

possible. The specific iterative process of the OMP algorithm in this paper is as follows:

(1) Input of signal $\boldsymbol{d}_{R_{\tilde{Y}}}$ and target dictionary $\boldsymbol{G}_{Y_T}$.
(2) Initialization of residual $\boldsymbol{r}=\boldsymbol{d}_{R_{\tilde{Y}}}$, projection vector $\gamma_I=0$, $\boldsymbol{I}=[]$, and $\boldsymbol{G}_I=[]$.
(3) Execute steps (4)–(7) when the number of iterations is not greater than N.
(4) Calculate the maximum inner product of each atom and residual in dictionary $\boldsymbol{G}_{Y_T}$, and get the corresponding atomic number $\hat{n}=\arg\max_n\left|(g^n)^T\boldsymbol{r}\right|$.
(5) Update $\boldsymbol{G}_I$ by $\boldsymbol{G}_I=[\boldsymbol{G}_I,\boldsymbol{G}_n]$.
(6) Sparse representation of computational signal $\boldsymbol{d}_{R_{\tilde{Y}}}$ in dictionary $\boldsymbol{G}_I$: $\gamma_I=\left(\boldsymbol{G}_I^T\boldsymbol{G}_I\right)^{-1}\boldsymbol{G}_I^T\boldsymbol{d}_{R_{\tilde{Y}}}$.
(7) Update $\boldsymbol{r}$ by $\boldsymbol{r}=\boldsymbol{r}-\boldsymbol{G}_I\gamma_I$.
(8) Terminate the iteration.
(9) Output subset $\boldsymbol{G}_I$ of target dictionary $\boldsymbol{G}_{Y_T}$, sparse projection vector γ_I of signal $\boldsymbol{d}_{R_{\tilde{Y}}}$ under dictionary.

In the previous section, the atoms of the target are preconstructed, the diagonal vectors of the auto-correlation matrix of several construction atoms are selected by OMP algorithm, and the corresponding matching coefficients (sparse representation) are calculated at the same time. Then the auto-correlation matrix of the selected atoms is used as the template, and the approximate auto-correlation matrix of the target is constructed by these templates and their corresponding matching coefficients. Finally, the eigen-decomposition values are calculated and the approximate Q-KLT basis of the target is obtained. The specific steps of constructing the approximate Q-KLT basis are as follows:

(1) The mixed signal $\tilde{\boldsymbol{y}}$ in slow time domain is receiv ed, and the mixed signal $\tilde{\boldsymbol{Y}}$ in Doppler domain is obtained by DFT.
(2) The auto-correlation matrix $\boldsymbol{R}_{\tilde{Y}}$ of mixed signal $\tilde{\boldsymbol{Y}}$ and the diagonal vector $\boldsymbol{d}_{R_{\tilde{Y}}}$ of $\boldsymbol{R}_{\tilde{Y}}$ are calculated.
(3) The OMP algorithm is used to iteratively calculate the signal $\boldsymbol{d}_{R_{\tilde{Y}}}$ and the target dictionary $\boldsymbol{G}_{Y_T}$. The atom $\bar{\boldsymbol{g}}_{Y_T}^{k_1},\bar{\boldsymbol{g}}_{Y_T}^{k_2},\ldots,\bar{\boldsymbol{g}}_{Y_T}^{k_j}$ matched by $\boldsymbol{d}_{R_{\tilde{Y}}}$ is selected from the target dictionary $\boldsymbol{G}_{Y_T}$, and the matching coefficient $\gamma_I=\left[\gamma_{k_1},\gamma_{k_2},\ldots,\gamma_{k_j}\right]$ is calculated.
(4) Select the atom corresponding to $\bar{\boldsymbol{g}}_{Y_T}^{k_1},\bar{\boldsymbol{g}}_{Y_T}^{k_2},\ldots,\bar{\boldsymbol{g}}_{Y_T}^{k_j}$ from dictionary $\boldsymbol{A}_{Y_T}$ and construct template $\overset{\frown}{R}_{Y_T}^{k_1},\overset{\frown}{\boldsymbol{R}}_{Y_T}^{k_2},\ldots,\overset{\frown}{\boldsymbol{R}}_{Y_T}^{k_j}$
$$\overset{\frown}{\boldsymbol{R}}_{Y_T}^{k_i}=\boldsymbol{a}_{Y_T}^{k_i}\left(\boldsymbol{a}_{Y_T}^{k_i}\right)^T,\quad i=1,2,\ldots,j. \tag{8}$$
(5) Calculating the approximate auto-correlation matrix $\boldsymbol{R}_{Y_T}=\sum_{i=1}^{j}\gamma_{k_i}\overset{\frown}{\boldsymbol{R}}_{Y_T}^{k_i}$ of $\boldsymbol{Y}_T$ according to the template and matching coefficients.
(6) Finally, $\boldsymbol{R}_{Y_T}=\boldsymbol{U}_{Y_T}^H\Lambda_{Y_T}\boldsymbol{U}_{Y_T}$ is obtained by eigen-decomposition of $\boldsymbol{R}_{Y_T}$, where $\boldsymbol{U}_{Y_T}^H$ and $\boldsymbol{U}_{Y_T}$ are orthogonal matrices, and Λ_{Y_T} is a diagonal matrix.

For convenience, we set the target signal as $\boldsymbol{Y}_T=\boldsymbol{Y}_1$ and set the jamming signal as $\boldsymbol{Y}_J=\boldsymbol{Y}_2$, then the approximate Q-KLT basis of the target is $\boldsymbol{U}_{Y_T}^H=\boldsymbol{U}_{Y_1}^H$ and the Q-KLT basis of the jamming signal is $\boldsymbol{U}_{Y_J}^H=\boldsymbol{U}_{Y_2}^H$.

Orthogonal transformation of signal $\boldsymbol{Y}_i(i=1,2)$ is defined as
$$\Theta_{Y_i}=\boldsymbol{U}_{Y_i}^H\boldsymbol{Y}_i. \tag{9}$$
Different from KLT basis, $\boldsymbol{U}_{Y_i}$ and $\boldsymbol{U}_{Y_i}^H$ are obtained by eigen-decomposition of auto-correlation matrix of signal $\boldsymbol{Y}_i$, which are only related to current signal $\boldsymbol{Y}_i$. To summarize, projection vector Θ_{Y_i} is the Q-KLT of signal $\boldsymbol{Y}_i$, and $\boldsymbol{U}_{Y_i}^H$ is the Q-KLT basis of $\boldsymbol{Y}_i$ signal.

C. Separation of target and jamming signal

In this section, BP algorithm is used to separate the mixed signals in Doppler domain. The basis of BP algorithm used l_1-norm to replace l_0-norm for convex optimization [13]. The steps of separation and reconstruction of mixed signals based on BP algorithm are given as follows:

(1) Calculating diagonal vector $\boldsymbol{d}_{R_{\tilde{Y}}}$ of auto-correlation matrix of mixed signal $\tilde{\boldsymbol{Y}}$.
(2) According to the algorithm in Section II, the Q-KLT basis $\boldsymbol{U}_{Y_2}^H$ of jamming signal $\boldsymbol{Y}_2$ is obtained, and the approximate Q-KLT basis $\boldsymbol{U}_{Y_1}^H$ of target $\boldsymbol{Y}_1$ is obtained with reference to $\boldsymbol{d}_{R_{\tilde{Y}}}$.
(3) By solving the following l_1-norm optimization problem:
$$\min f(\beta_1,\beta_2)=\min\sum_{i=1}^{2}\|\beta_i\|_1,\quad s.t.\ \tilde{\boldsymbol{Y}}=\sum_{i=1}^{2}\boldsymbol{U}_{Y_i}\beta_i, \tag{10}$$
we get the estimated Θ_{Y_i} of sparse representation of $\boldsymbol{Y}_i$ under $\boldsymbol{U}_{Y_i}$, where $\beta^{opt}=[\Theta_{Y_1},\Theta_{Y_2}]^T$ is the optimal solution of problem (10).
(4) The separated echo PC signal $\hat{\boldsymbol{Y}}_i$ is obtained by the following reconstruction:
$$\hat{\boldsymbol{Y}}_i=\boldsymbol{U}_{Y_i}\Theta_{Y_i},\quad i=1,2 \tag{11}$$

IV. SIMULATION AND MEASUREMENT RESULTS

In simulation, the radar works in X-band, the PRI is 100 US, and M = N = 128 is assumed. In this section, we verify the feasibility of dual channel processing to obtain the Doppler information of false targets; then assume that we can verify the effectiveness and superiority of the anti-strong velocity jamming in three scenarios.

First, single target corresponds to single false target (1T-1F) scene, $f_T = 0.6$ and $f_J = 0.62$. Second, single target corresponds to three false target (1T-3F) scenarios, $f_T = 0.6$ and $f_J = 0.58$, 0.62, and 0.78. Third, four targets correspond to eight false targets (4T-8F) scenarios, $f_T = 0.2$, 0.4, 0.6, and 0.8 and $f_J = 0.18$, 0.22, 0.38, 0.42, 0.58, 0.62, 0.78, and 0.82. We set signal-to-noise ratio (SNR) = 10 dB and jamming-to-signal ratio (JSR) = 20 dB.

In the 1T-1F scenario, it is assumed that the number of PRIs of jamming lagging transmission signal is 30, namely $i = 30$. It can be seen from the numerical simulation that the radian value of 30 sampling points is 1.16 (rad), which is twice the radian value of other sampling points. According to the analysis in Section II, the proposed peak detection can estimate i value as 30, as shown in Figure 3. After the i value is determined, the Doppler information of the jamming is obtained by the dual channel processing. As shown in Figure 4, due to the high jamming intensity, the target peaks of the output results of channel 1 are completely covered by the raised noise base, while the output of channel 2 have three large peaks, corresponding to the Doppler frequencies of 0.58, 0.62, and 0.78, respectively.

In the 1T-3F and 4T-8F scenarios, the effectiveness of the new method is verified. Then, in those three scenarios, peak sidelobe ratio (PSLR) after jamming suppression is used to measure the proposed anti-jamming method.

1T-3F scene: As shown in Figure 5, when there is jamming, the anti-jamming signal has the same main lobe as the target echo (no jamming) after coherent processing. Although the sidelobes of these two signals are slightly different, they do not affect the detection of single target. Therefore, the method has a good effect in suppressing strong jamming, while the traditional method of correlation processing (CP) cannot eliminate the influence of high sidelobe on target concealment. As shown in Figure 6, the projection vectors of jamming and target signals on Q-KLT basis are obtained. It can be found that the projection vector of the jamming signal in the graph has only one large amplitude, and the amplitude of other sampling points is approximately zero. From the enlarged figure, it can be seen that the projection vector of the target has only one large amplitude. It is verified that the jamming and target signal have good sparseness in the adaptive dictionary; so the effectiveness of this paper is verified in the single target and strong jamming scenarios.

4T-8F scene: Figure 7 showed that the four main lobes of the separated target are the same as the main lobes of the target echo (no jamming) after coherent processing.

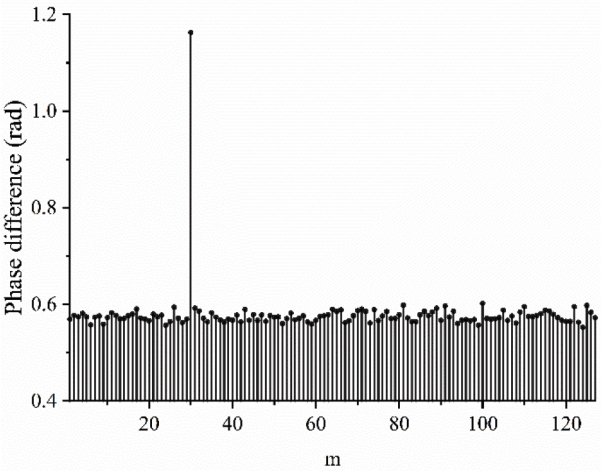

Fig. 3. Estimation of delay number i of jamming signal.

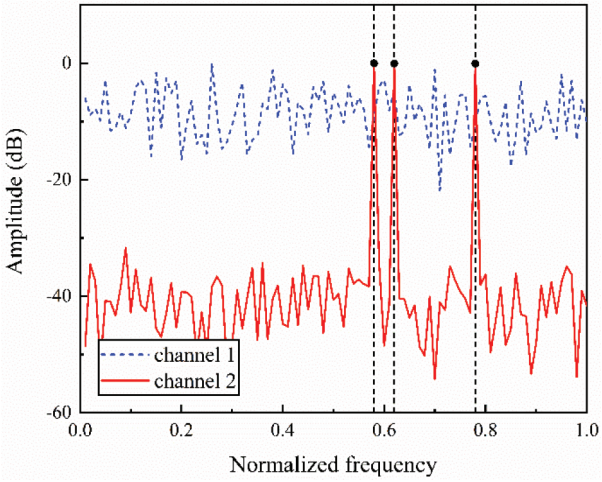

Fig. 4. Simulation of dual channel processing.

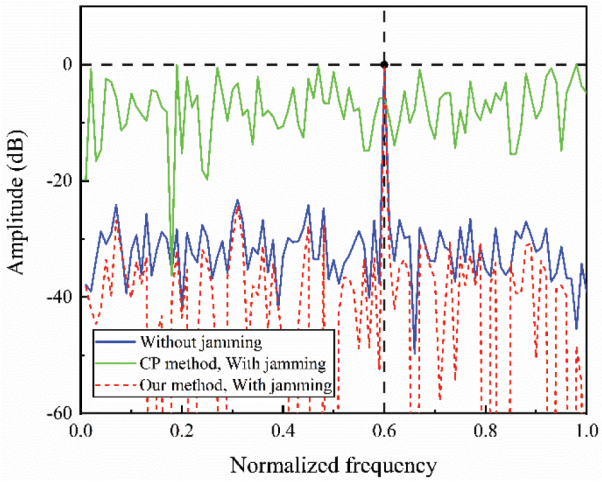

Fig. 5. Jamming suppression in 1T-3F scene.

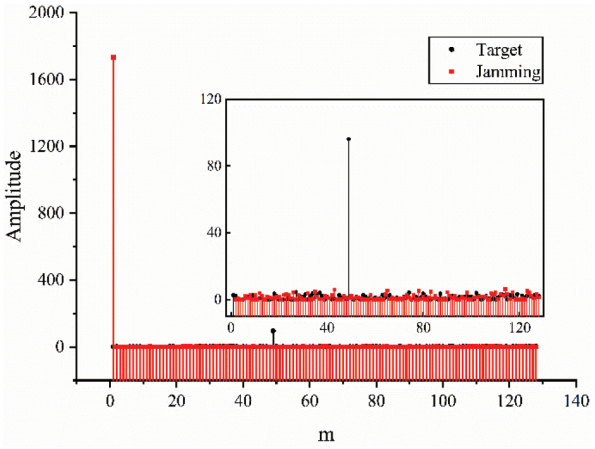

Fig. 6. Projection vector in 1T-3F scene.

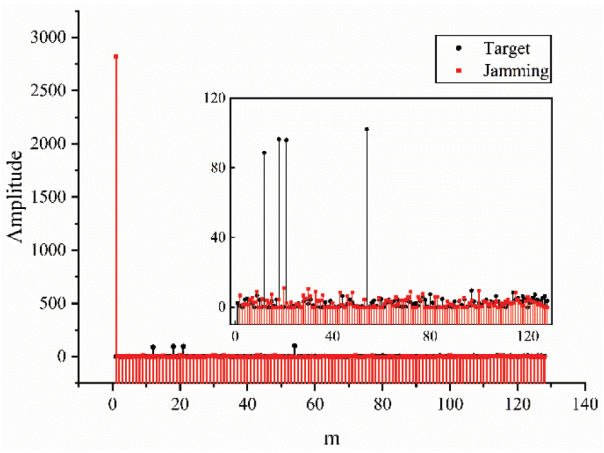

Fig. 8. Projection vector in 4T-8F scene.

It is verified that our method has good anti-jamming performance in four target scenarios, but the CP method cannot detect the target at all. As shown in Figure 8, the projection vectors of jamming and target signals on Q-KLT basis are obtained. It is found that the projection vector of jamming signal has only one large amplitude, while the projection vector of target signal has four large amplitudes. It is verified that the jamming and target signal have good sparsity in the adaptive dictionary, so that the effectiveness of method proposed in this paper is verified in the multi-target and strong jamming scenarios.

To verify the effect of different JSR and SNR on PSLR, Figure 9 showed the simulation results of 1000 independent trials for Monte Carlo simulations. In Figure 9(a), the PSLR in the three scenarios remains unchanged with the increase of JSR, and the PSLR values in 1T-1F and 1T-3F scenarios are nearly the same,

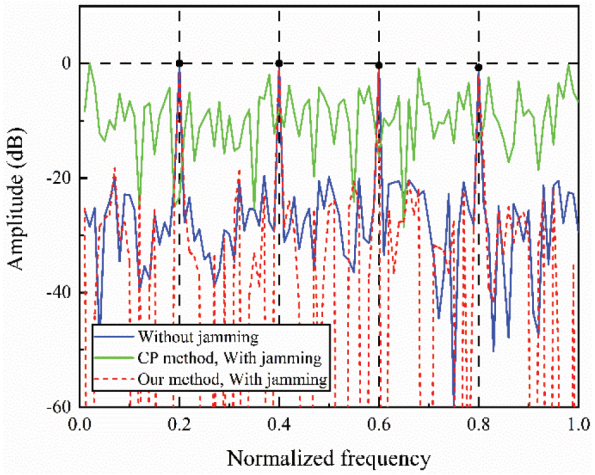

Fig. 7. Jamming suppression in 4T-8F scene.

while the PSLR values in 4T-8F scenarios are slightly less than the above two scenarios, which indicates that the change of JSR will not affect the jamming suppression performance of this method. In Figure 9(b), PSLR in the three scenarios increases with the increase of SNR, and the increase degree of PSLR in 1T-1F and 1T-3F scenarios is the identical, while the increase of PSLR in 4T-8F scenario is slower under the condition of low SNR.

Furthermore, the simulation verifies the effect of the number of N on the performance of this method. It can be seen from Table 1 that in the 1T-3F and 4T-8F scenarios, the increase of N value will reduce the PSLR value. From formula (3), it can be seen that the increase of N can improve the velocity resolution, but also increase of the number of atoms in the pre-constructed target signal dictionary, which not only improves the calculation but also reduces the jamming suppression performance. In Figure 10, for example, $N = 2M$, red and blue dashed lines show that PSLR value increases with the increase of SNR, but the increase rate slows down.

Finally, the method proposed is compared with the adaptive sequence estimation (ASE) algorithm in [14] to further verify its superiority. In [14], in a single target scenario, the noise power is $|\sigma_N|^2 = 0$ dB, the power of the jamming signal is set to $|\sigma_J|^2 = 40$ dB, and the power of the target signal $|\sigma_T|^2$ is set to 0, 10, 20, 30, and 40 dB, respectively. Under the condition of the same parameters above, 1000 independent trials for Monte Carlo simulations are carried out. Figure 11 shows the PSLR values of ASE method and this method under different target signal powers. It can be found that the PSLR value of this method is greater than ASE method under each target power, which proves that this method has better performance in suppressing velocity jamming. For the future application, the adaptive methods can also

Table 1: PSLR values corresponding to different N numbers (SNR = 10 dB)

N numbers	1T-3F scene	4T-8F scene
N= M	24.53 dB	18.27 dB
N= 2M	21.98 dB	15.20 dB
N= 3M	21.28 dB	14.60 dB
N= 4M	21.16 dB	14.36 dB

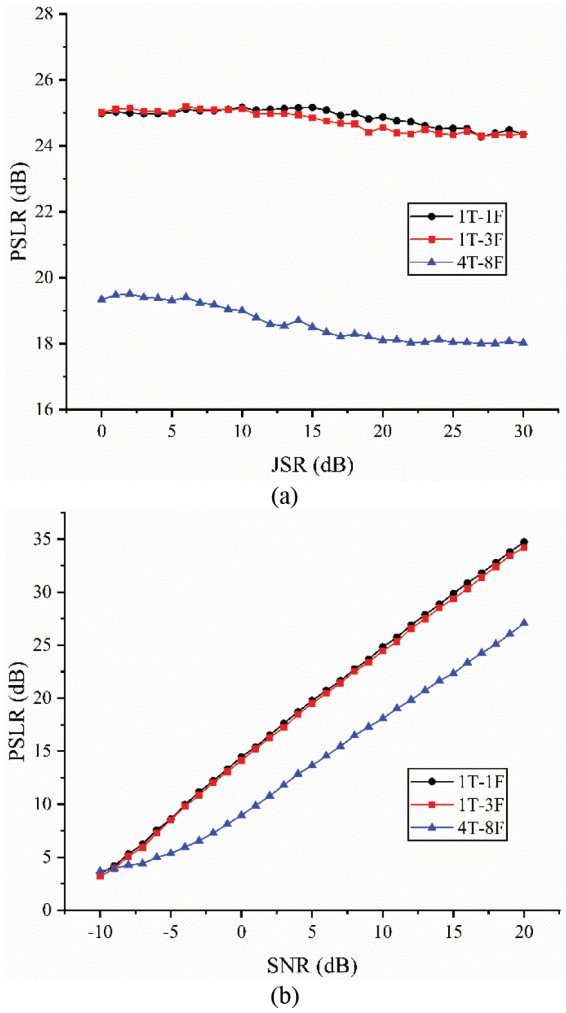

Fig. 9. PSLR after jamming suppression versus (a) JSR and (b) SNR.

be considered in the interference suppression [15–18]. In addition, the adaptive interference suppression for PD radar can be considered using adaptive filtering [19–28] and sparse arrays [29–31].

V. CONCLUSION

Because the RPIP waveform is affected by the raised noise base and cannot give full play to the efficiency of restraining the deception, the detection performance of

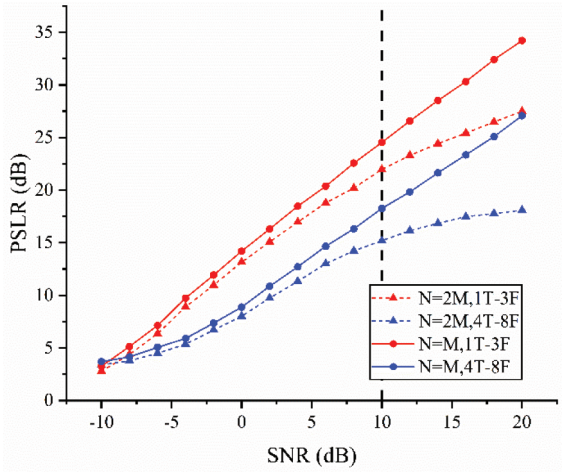

Fig. 10. Number N impact on the PSLR.

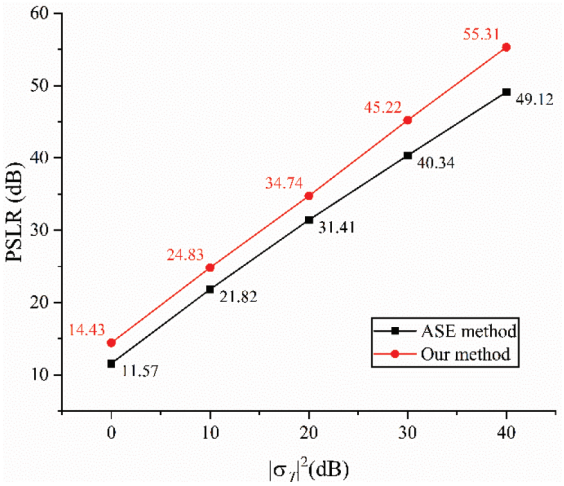

Fig. 11. PSLR performance comparison of the two methods.

PD radar is seriously damaged under the strong velocity jamming. To solve this problem, a new anti-jamming method based on adaptive dictionary is proposed by combining traditional CP technology with sparse decomposition theory. The prior knowledge is acquired by dual channel processing, and then the Q-KLT basis of jamming a target is constructed, so that the signal has good sparsity under adaptive dictionary. The superiority of the method under the condition of strong jamming is studied by numerical simulation. The results show that the change of the jamming signal strength has little influence on the algorithm performance, which means that this method can effectively suppress the jamming of strong velocity deception. In addition, this method can reduce Doppler sidelobe and has better anti-jamming performance, compared with ASE method.

ACKNOWLEDGMENT

This paper is supported by Shanghai Aerospace Science and Technology Innovation Fund under Grant SAST2019-002.

REFERENCES

[1] J. Dudczyk, "Radar emission sources identification based on hierarchical agglomerative clustering for large data sets," *J. Sens.*, vol. 2016, pp. 1-9, 2016.

[2] J. Dudczyk, "A method of feature selection in the aspect of specific identification of radar signals," *Bull. Polish Acad. Sci. Tech. Sci.*, vol. 65, pp. 113-119, 2017.

[3] N. Li and Y. Zhang, "A survey of radar ECM and ECCM," *IEEE Trans. Aerosp. Electron. Syst.*, vol. 31, no. 3, pp. 1110-1120, 1995.

[4] S. Roome, "Digital radio frequency memory," *IEE Electron. Commun. Engng J.*, vol. 2, no. 4, pp. 147-153, 1990.

[5] S.D. Berger and D.E. Meer, "An expression for the frequency spectrum of a digital radio frequency memory signal," IEEE National Aerospace Electronics Conf., Dayton, OH, pp. 90-93, May 1990.

[6] S.D. Berger, "Digital radio frequency memory linear range gate stealer spectrum," *IEEE Trans. Aerosp. Electron. Syst.*, vol. 39, no. 2, pp. 725-735, 2003.

[7] L. Ding, R. Li, Y. Wang, L. Dai, and F. Chen, "Discrimination and identification between mainlobe repeater jamming and target echo by basis pursuit," *IET Radar Sonar Navig.*, vol. 11, no. 1, pp. 11-20, 2017.

[8] J. Sui, Z. Liu, X. Wei, X. Li, B. Peng, and D. Liao, "Velocity false target identification in random pulse initial phase radar based on compressed sensing," 2015 3rd International Workshop on Compressed Sensing Theory and its Applications to Radar, Sonar and Remote Sensing (CoSeRa), Pisa, pp. 179-183, 2015.

[9] Z. Liu, J. Sui, Z. Wei, and X. Li, "A sparse-driven anti-velocity deception jamming strategy based on pulse-doppler radar with random pulse initial phases," *Sensors*, vol. 18, no. 4, 1249, 2018.

[10] J. Zhang, D. Zhu, and G. Zhang, "New antivelocity deception jamming technique using pulses with adaptive initial phases," *IEEE Trans. Aerosp. Electron. Syst.*, vol. 9, no. 2, pp. 1290-1300, 2013.

[11] J. Sui, X. Zhang, Z. Liu, X. Wei, and X. Li, "Sparse-based false target identification in pulse-doppler radar with random pulse initial phase," 2015 International Conference on Wireless Communications & Signal Processing (WCSP), Nanjing, pp. 1-5, 2015.

[12] Y. Pati, R. Rezaiifar, and P. Krishnaprasad, "Orthogonal matching pursuit: recursive function approximation with applications to wavelet decomposition," Proceedings of 27th Asilomar Conference on Signals, Systems and Computers, Pacific Grove, CA, USA, vol. 1, pp. 40-44, 1993.

[13] S. Chen, D. Donoho, and A. Saunders, "Atomic decomposition by basis pursuit," *SIAM Rev.*, vol. 43, no. 1, pp. 129–159, 2001.

[14] G. Cui, H. Ji, V. Carotenuto, S. Iommelli, and X. Yu, "An adaptive sequential estimation algorithm for velocity jamming suppression," *Signal Process.*, vol. 134, pp. 70-75, 2017.

[15] Z. Dai, L. Guo, J. Yin, Y. Li, and K. Guo, "Adaptive sparse array beamforming using correntropy induced metric constrained normalized LMS algorithm," *Applied Computational Electromagnetics Society (ACES) Journal*, vol. 35, no. 4, pp. 430-436, 2020.

[16] W. Shi and Y. Li, "A p-norm-like constraint LMS algorithm for sparse adaptive beamforming," *Applied Computational Electromagnetics Society (ACES) Journal*, vol. 34, no. 12, pp. 1797-1803, 2019.

[17] W. Shi, Y. Li, and J. Yin, "Improved constraint NLMS algorithm for sparse adaptive array beamforming control applications," *Applied Computational Electromagnetics Society (ACES) Journal*, vol. 34, no. 3, pp. 419-424, 2019.

[18] W. Li, X. Mao, Z. Zhai, and Y. Li, "A low complexity high performance robust adaptive beamforming," *Applied Computational Electromagnetics Society (ACES) Journal*, vol. 32, no. 5, pp. 441-448, 2017.

[19] Y. Li, Z. Jiang, W. Shi, X. Han, and B. Chen, "Blocked maximum correntropy criterion algorithm for cluster-sparse system identifications," *IEEE Trans. Circuits Syst. II, Express Briefs*, vol. 66, no. 11, pp. 1915-1919, Nov. 2019.

[20] W. Shi, Y. Li, and Y. Wang, "Noise-free maximum correntropy criterion algorithm in non-Gaussian environment," *IEEE Trans. Circuits Syst. II Express Briefs*, vol. 67, no. 10, pp. 2224-2228, Oct. 2020.

[21] W. Shi, Y. Li, and B. Chen, "A separable maximum correntropy adaptive algorithm," *IEEE Trans. Circuits Syst. II, Express Briefs*, vol. 67, no. 11, pp. 2797-2801, Nov. 2020.

[22] Y. Li, Y. Wang, and T. Jiang, "Norm-adaption penalized least mean square/fourth algorithm for sparse channel estimation," *Signal Processing*, vol. 128, pp. 243-251, 2016.

[23] X. Huang, Y. Li, Y. V. Zakharow, Y. Li, and B. Chen, "Affine-projection Lorentzian algorithm for vehicle hands-free echo cancellation," *IEEE Transactions on Vehicular Technology*, vol. 70, no. 3, pp. 2561-2575, 2021.

[24] T. Liang, Y. Li, W. Xue, Y. Li, and T. Jiang, "Performance and analysis of recursive constrained least Lncosh algorithm under impulsive noises," *IEEE*

Transactions on Circuits and Systems II: Express Briefs, vol. 68, no. 7, pp. 2217-2221, 2021.
[25] T. Liang, Y. Li, Y. V. Zakhrow, W. Xue, and J. Qi, "Constrained least Lncosh adaptive filtering algorithm," *Signal Processing*, vol. 183, 2021.
[26] T. Liang, Y. Li, and Y. Xia, "Recursive Constrained Adaptive Algorithm under q-R'enyi Kernel Function," *IEEE Transactions on Circuits and Systems II: Express Briefs*, vol. 68, no. 6, pp. 2227-2231, 2021.
[27] Q. Wu, Y. Li, Y. Zakharov, W. Xue, "Quantized kernel least lncosh algorithm," *Signal Processing*, vol. 189, ID:108255, 2021.
[28] Y. Li and Y. Wang, "Sparse SM-NLMS algorithm based on correntropy criterion," *Electronics Letters*, vol. 52, no. 17, pp. 1461-1463, 2016.
[29] Y. Li, C. Zhang, and S. Wang, "Low-complexity non-uniform penalized affine projection algorithm for sparse system identification," *Circuits, Systems,and Signal Processing*, vol. 35, no. 5, pp. 1611-1624, 2016.
[30] W. Shi, S. A. Vorobyov, and Y. Li, "ULA fitting for sparse array design," *IEEE Transactions on Signal Processing*, vol. 69, pp. 6431-6447, 2021.
[31] W. Shi, Y. Li, and S. A. Vorobyov, "Low mutual coupling sparse array design using ULA fitting," 2021 IEEE International Conference on Acoustics, Speech and Signal Processing (ICASSP), Toronto, ON, Canada, 13 May, 2021.

Zhe Du received the B.S. degree from Qing Dao University in 2010 and the M.S. degree from Shanghai University in 2013.

He works with Shanghai Electro-Mechanical Engineering Institute as a Senior Engineer. His research interests include electromagnetic compatibility, complex system simulation and evaluation, antenna theory, and design.

Lexin Yu received the B.S. degree from the School of Electronics and Information Engineering, Tianjin Polytechnic University in 2017 and the M.S. degree from the School of Information and Communication Engineering, Harbin Engineering University in 2021.

After studies, he worked with Huawei Company, China, as an Applications Engineer. His research interests include modeling and simulation, and anti-jamming technology.

Jin Zhang received the B.S. degree from the School of Astronautics, Northwestern Polytechnical University in 2016 and the M.S. degree from the School of Astronautics, Northwestern Polytechnical University in 2019.

She works with Shanghai Electro-Mechanical Engineering Institute as an Applications Engineer. Her research interests include electronic modeling and simulation, and guidance and control system design for flight vehicles.

Tao Jiang received the Ph.D. degree from the Harbin Engineering University, Harbin, China, in 2002.

Since 1994, he has been a Faculty Member of College of Information and Communication, Harbin Engineering University, where he is currently a Professor. He was a Postdoctoral Researcher with the Research Institute of Telecommunication, Harbin Institute of Technology, Harbin, China, from 2002 to 2003, and a Visiting Scholar with the Radar Signal Processing Laboratory, National University of Singapore, from 2003 to 2004. His current research interests include radio wave propagation, complex electromagnetic system evaluation, modeling, and simulation.

Mingjuan Cai received the Ph.D degree from National University of Defence Technology, Changsha, China, in 2006. She works with Naval Research Academy as a Senior Engineer. Her current research interests include electromagnetic simulation, electromagnetic compatibility and evaluation.